Wireless LLC converter for electric bicycle

Alberto M. Pernía[1], Miguel J. Prieto[1], Juan A. Martín-Ramos[1], Pedro J. Villegas[1]
Alberto Navarro[2], Javier Sedano[2].

Área de Tecnología Electrónica, Universidad de Oviedo, Spain
[2]Institute of Technology of Castilla y Leon, ITCL

2020 IEEE Vehicle Power and Propulsion Conference (VPPC) | 978-1-7281-8959-8/20/$31.00 ©2020 IEEE | DOI: 10.1109/VPPC49601.2020.9330839

***Abstract*— We are in a process of evolution and change in terms of transportation methods, especially in cities. The electric vehicle is beginning to be a tangible reality that we can find in all our cities. The reduction of pollution in increasingly populated cities suggests a transformation process by which combustion-based vehicles will give way to less polluting vehicles. In this transformation process we cannot forget about new transport systems such as the electric bicycle or scooter. They are portable elements of limited power and widely used in the population for short trips. Currently the vast majority of chargers used are direct contact. In order to reduce maintenance and increase user's comfort, the use of a wireless charger based on the LLC resonant topology is proposed**

***Index Terms*— Resonant converter, LLC topology, soft switching, battery charger, electric vehicle.**

I. Introduction

A 40% reduction in greenhouse gases is one of the key objectives for 2030. The achievement of this objective involves the use of renewable energy. Currently there is significant pressure from the social agents that are forcing automotive companies to rapidly evolve towards the electric car, assuming that this type of vehicle produces zero emissions. Although there are different opinions about this idea, the fact is that the electric vehicle is a reality nowadays and a possible way to reduce the pollution in our cities.

A major challenge that electric vehicle manufacturers face is the charging process. In the case of the electric car the problem is exacerbated due to the required autonomy and the necessary charging times. To a lesser extent other types of electric vehicles, such as bicycles or scooters, present a similar problem.

The main advantage in this case is the lower autonomy and shorter usage times throughout the day, which makes it possible to avoid fast charges. On the contrary, during the waiting times, partial charges can be made that allow a high state of charge in the battery in most of the occasions.

The chargers are traditionally designed so that direct contact with the vehicle is made through a connector with a low contact resistance [1-2].

This approach facilitates the design but incorporates some inconvenience derived from the maintenance of the contacts that deteriorate with use.

Another aspect to consider is user's comfort. In this sense, wireless chargers are already spreading in other sectors such as mobile devices. The forecast is to increase its use also in applications related to personal mobility.

Although the comfort provided by a wireless charging process is clear, we cannot forget some drawbacks associated with this type of technology. Some of them are the greater complexity in the design, possible performance penalty and a higher emission of electromagnetic radiation that must be controlled to comply with the EMC regulations.

The presence of these drawbacks does not imply an insoluble limitation and there are several approaches depending on the application and power of the charger.

The general scheme followed in the wireless chargers is the one shown in figure 1.

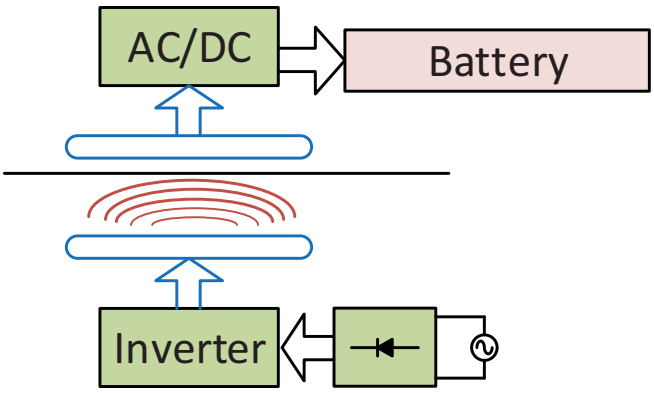

Fig.1. Basic wireless charger scheme.

In general, we can mention that the selection of the power topology to use depends largely on the design of the wireless coupling. This coupling is typically performed using magnetic fields, although we can also find devices based on capacitive coupling [3-4].

Focusing on the magnetic coupling, the geometry of the coupled coils will define the particular characteristics of their operation. In order to characterize this operation, electrical models of greater or lesser complexity will be used, where two

978-1-7281-8959-8/20/$31.00 ©2020 IEEE

fundamental elements will always stand out: the leakage inductance (Ld) and the magnetizing inductance (Lm).

Due to the distance between the primary and secondary windings, which can be tens of millimetres, the leakage inductance (Ld) will have values comparable to or even greater than the magnetizing inductance. The leakage inductance compensation technique involves the inclusion of a resonant capacitor (Cr) in series with the leakage inductance, which typically is the resonant inductance (Lr) of the circuit (fig. 2).

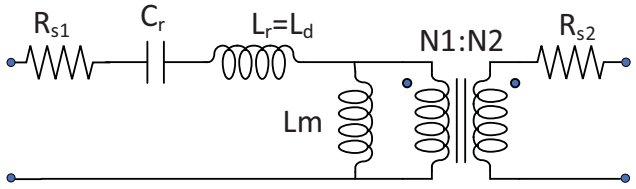

Fig.2. Compensation topology

As a consequence of the high existing leakage inductance, it is usually not necessary to increase this value with an additional coil, so the resonant inductance usually coincides with the leakage inductance.

From the model presented in figure 2 a LLC resonant topology follows directly.

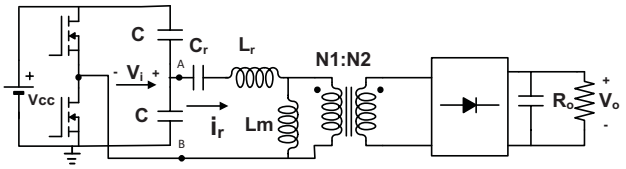

Fig.3. LLC resonant topology

The LLC resonant topology shown in Figure 3 shows an input voltage that will come from the rectified and filtered mains voltage to achieve a constant value represented by Vcc. In this figure a half bridge has been represented although the mathematical analysis does not differ in the case of using a full bridge.

II. Circuit Analysis

A. Circuit Model

To simplify the mathematical analysis [5], we can model the LLC converter using the first harmonic (Vi1) of the voltage generated in the inverter bridge Vi (Fig.4).

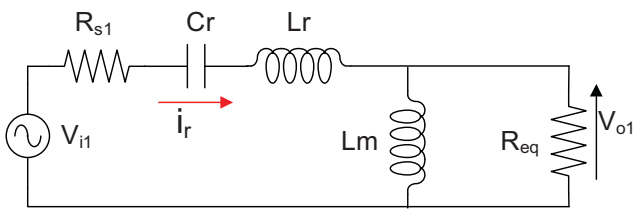

Fig. 4. First harmonic approximation

The equivalent resistance [3] referred to the primary is defined by the mathematical expression (1)

$$R_{eq} = \frac{8}{\pi^2} \cdot \left(\frac{N1}{N2}\right)^2 \cdot Ro \tag{1}$$

Therefore, the circuit is reduced to a series impedance defined by the capacitor and the resonant inductance (Zs) and a parallel impedance (Zp) defined by the equivalent load and the magnetizing inductance.

$$Z_s = Rs1 + \frac{1}{jwC_r} + jwL_r \tag{2}$$

$$Z_p = \frac{1}{\frac{1}{jwLp} + jwC_p + \frac{1}{Req}} \tag{3}$$

The parallel winding capacitance Cp can be negligible in this type of wireless transformer. The conversion ratio of the LLC topology can be calculated from the impedances

$$M = \frac{V_o}{V_i} = \frac{Z_p}{Z_p + Z_s} \tag{4}$$

Defining:

$$f_n = \frac{f_s}{f_r} \tag{5}$$

$$L_n = \frac{L_m}{L_r} \tag{6}$$

$$Q = \frac{\sqrt{\left(L_r/C_r\right)}}{R_{eq}} \tag{7}$$

Equation (4) can be transformed in:

$$M = \frac{L_n \cdot f_n^2}{\left[(L_n+1)\cdot f_n^2 - 1\right] + j\left[\left(f_n^2-1\right)\cdot f_n \cdot Q \cdot L_n\right]} \tag{8}$$

Once we have the conversion ratio, the design of the charger will depend on the Q and Ln values. In a traditional design where the transformer does not have the restrictions of a wireless transformer, the Ln range is typically selected from 3 to 9. The parameter Q allows to obtain a peak gain higher than the maximum resonant gain required to compensate the power losses in the converter. A common value for Q can be 0.5.

B. Topology design

The first parameter that we must define in the converter is the turn ratio of the wireless transformer and for this we will assume a conversion ratio of the LLC topology M = 1 to reduce the electrical stress (Fig. 5) [6-10].

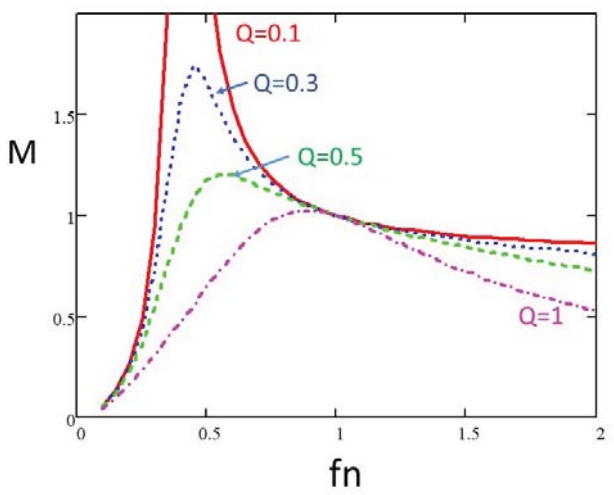

Fig. 5. Conversion ratio of the LLC resonant topology

Then, we can assign:

$$n = \frac{N1}{N2} = \frac{Vcc}{2 \cdot Vo} \quad (9)$$

If the input voltage to the converter comes from the main ac rectified and filtered, we can assume Vcc = 325V.

Focusing on the problem of an electric bicycle charger, and more specifically on the bicycle model in which the battery is distributed on the rear wheel, figure 6, the external charger will have to supply a constant voltage between Vo=36-40V.

The rear wheel includes a set of battery management systems (BMS) to control the quality of the charging process and the protection of the batteries.

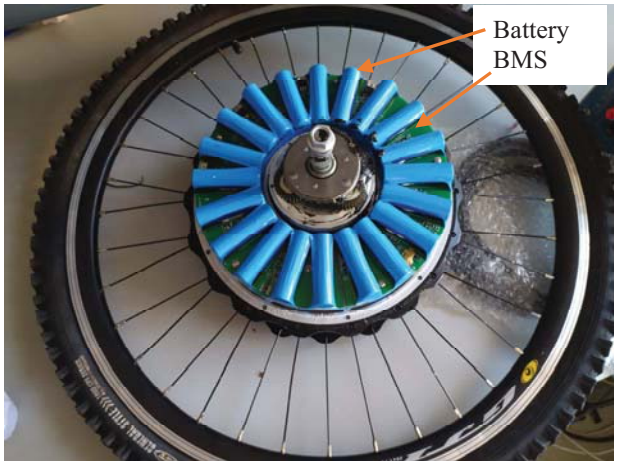

Fig. 6. Rear wheel

The battery used is a lithiun ion battery 36V-2.9 Ah.
Then, we can assign the wireless transformer a turn ratio of n=5. Once we define the transformer ratio, the relation between magnetizing and leakage inductance typically is assumed to be at least Ln=5.

With this information we can go to the curves shown in figure 5 and obtain the value of Q that allows us to find the conversion ratio M. Since the power losses present in the converter will reduce the effective value of M, we will tend to choose a value of Q that increases the conversion ratio of the converter by 10%

Then, with these premises Q = 0.45 is selected. Once the converter's working frequency has been selected, the rest of the parameters are defined. Thus, if fr = 200kHz the resonant elements would take the values: Lr=100µH, Lm=500 µH, Cr=6nF, Req=280Ω.

These values can be used to simulate the behaviour of the converter, to check its operation and observe how the specified output voltage is reached.

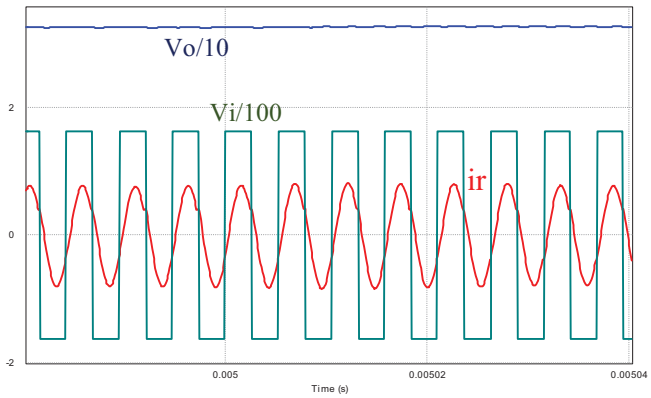

Fig. 7. Simulation results of a LLC converter

The main problem with the previous design is that it does not take into account the physical restrictions that accompany the wireless transformer. In order to replace the current contact charging systems present in some of our cities, such as the one shown in figure 8, an effective surface is specified for the 100x100 mm wireless transformer.

Fig. 8. Charging station in Madrid (Spain)

The design of the transformer becomes the priority parameter, conditioning the values of the resonant and magnetizing inductance. With the surface assigned for the primary, a prototype of flat windings is built on ferrites EPCOS B66295K0000X187 - I, I64/5/50, material N87 (Fig. 9).

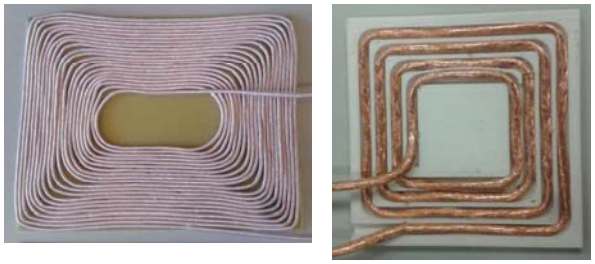

Fig. 9. Primary (left: 12x10 cm) and secondary windings (right: 10x10cm)

The distance between windings is another parameter to take into account since it conditions the value of both Lr and Lm. Although this distance will be an adjustable parameter, d=10 mm is initially taken as reference. Finally, the complete transformer is shown in figure 10.

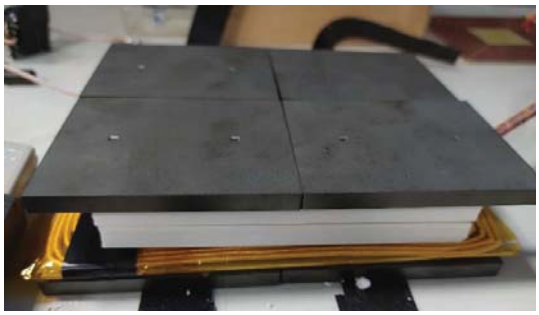

Fig. 10. Wireless transformer (13x10 cm)

Using the HP4194 impedance analyser, the transformer can be characterized according to the distance from the windings (Fig. 11)

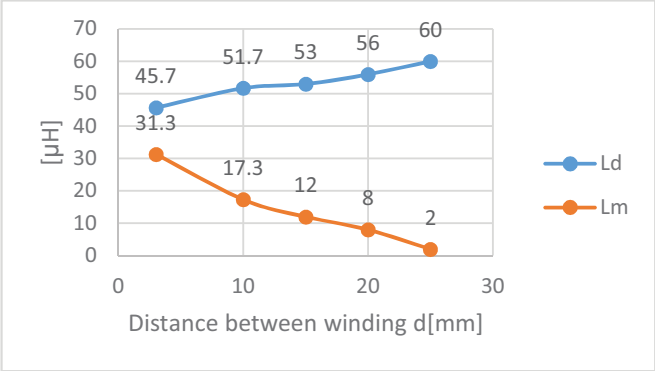

Fig. 11. Magnetizing and leakage inductance variation with distance

The reduction of the magnetizing inductance penalizes the performance of the converter by increasing the current through the primary and reducing the output voltage. The design of the converter now involves adjusting the rest of the parameters used depending on the transformer obtained.

Therefore, taking as values Lr = 45uH and Lm = 30uH the relation between both elements defines Ln = 0.66. To achieve a conversion ratio in the topology close to M = 1.5, the value of the quality factor will be Q = 0.75. From equation (7) a value of the resonant capacitor Cr = 1nF can be determined and therefore the resonance frequency takes the value:

$$f_r = \frac{1}{2\pi \cdot \sqrt{(L_r \cdot C_r)}} = 750kHz \tag{10}$$

This relatively high frequency may be achievable but may also penalize the efficiency of the converter. Assuming the use of serial low resistance SiC switches in order to minimize both conduction and switching losses, the power dissipation in the transformer is highly conditioned by this frequency.

Increasing the switching frequency reduces the current through the primary due to a higher impedance in the magnetizing inductance but increases the losses in the magnetic material.

To analyse the losses in the transformer, the model in figure 4 can be used. In it, the current flowing through the magnetizing inductance, can be determined versus frequency, and the current through Req depends on the output voltage. Therefore, we can calculate the value of the current through the resonant elements (Lr, Cr) with the previous information.

$$\overrightarrow{i_r} = \overrightarrow{i_{Lm}} + \overrightarrow{i_{Req}} \tag{11}$$

The calculation of i_r allows us to determine the conduction losses in the transformer (Pr) which also depend on the switching frequency, these losses are reduced when frequency increases because of the higher impedance of Lm.

$$Pr = Rs1 \cdot \left[\left(\frac{Vo \cdot \pi}{2\sqrt{2} \cdot Ro \cdot n}\right)^2 + \left(\frac{2\sqrt{2} \cdot Vo \cdot n}{2\pi^2 \cdot f \cdot Lm}\right)^2\right] + Rs2 \cdot \left(\frac{Vo \cdot \pi}{2\sqrt{2} \cdot Ro}\right)^2 \tag{12}$$

Rs1 and Rs2 represent the primary and secondary series resistance of the transformer.

By calculating the reluctance of the magnetic path, the magnetic field handled by the ferrite can be estimated. This magnetic field, close to B=50mT, determines the core losses (Pn) versus frequency, which can be derived from correlation (13) calculated with the data of the manufacturer, and which provides an accuracy of R=0.99 (from Excel).

$$Pn = 0.0005 \cdot f^2 + 0.277 \cdot f - 6.0146 \quad [kW/m^3] \tag{13}$$

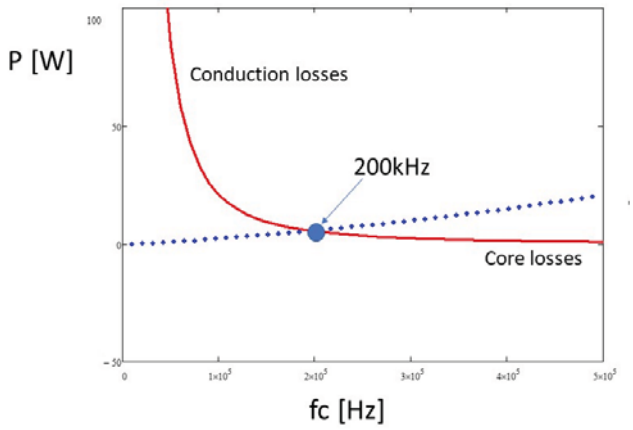

Fig. 12. Power losses in the wireless transformer

Then, to optimize the losses in the transformer we can select the resonance frequency fr = 200kHz (Fig. 12). The leakage

inductance is fixed by the wireless transformer and using equation (10) the new resonant capacitor will be Cr=14nF. The rest of the parameters are derived from equations (5) to (7): Ln=0.66, Q=0.2. With this data and expression (8) the conversion gain can be plotted (Fig. 13):

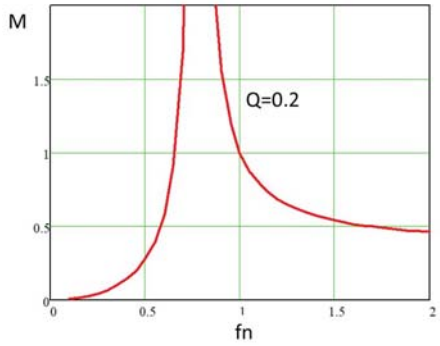

Fig. 13. Conversion ratio with Q=0.2,

III. Experimental Results

The prototype built for the verification of the theoretical results differs slightly from the scheme shown in Fig. 3 since the capacitors C have been eliminated, connecting terminal A to the middle point of the transistor leg and terminal B to ground (Fig. 14). The resonant capacitor Cr is now the component that eliminates the DC voltage from the wireless transformer

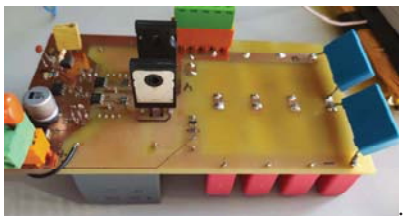

Fig. 14. LCC resonant converter prototype

The experimental results obtained show that the output voltage is easily achievable due to the high gain that the circuit presents with small frequency variations (Fig. 15)

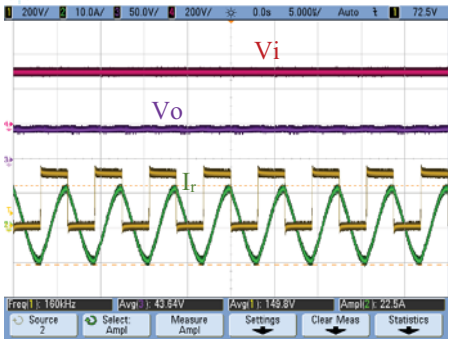

Fig. 15. LCC resonant converter waveforms

SiC switches (SCT3060ALGC11) of 60mΩ-650V have been used. The tests carried out with resistive loads show an output voltage variation of 10% when varying the distance from 5 to 15 mm and also the load Ro from 15 to 23 ohms [11]. Due to the redesign required by the inductance values of Lr and Lm obtained in the transformer, the switches withstand greater electrical stress. The efficiency obtained in the experimental result reaches 90%

IV. Conclusion

The increase in the use of individual electric vehicles such as bicycles or scooters also causes a greater demand for charging points. To improve user's comfort, wireless charging processes are seen as an efficient alternative. The resonant LLC topology is an efficient alternative to achieve the leakage inductance compensation of the wireless transformer. Finally, experimental results have been obtained that confirm the capability to get the specified output voltage under load variations with an efficiency of 90%

Acknowledgment

This work was supported by the Institute of Technology of Castilla y Leon, ITCL

References

[1] H. H. Wu, A. Gilchrist, K. Sealy, P. Israelsen, y J. Muhs, «A review on inductive charging for electric vehicles», en 2011 IEEE International Electric Machines Drives Conference (IEMDC), may 2011, pp. 143-147, doi: 10.1109/IEMDC.2011.5994820.

[2] M. P. Kazmierkowski y A. J. Moradewicz, «Contactless energy transfer (CET) systems #x2014; A review», en 2012 15th International Power Electronics and Motion Control Conference (EPE/PEMC), sep. 2012, p. Session 3-1-Session 3-6, doi: 10.1109/EPEPEMC.2012.6397378

[3] C.-S. Wang, O. H. Stielau, y G. A. Covic, « C.-S. Wang, O. H. Stielau, y G. A. Covic, «Design considerations for a contactless electric vehicle battery charger», IEEE Transactions on Industrial Electronics, vol. 52, n.º 5, pp. 1308-1314, oct. 2005, doi: 10.1109/TIE.2005.855672.

[4] Z. Li, C. Zhu, J. Jiang, K. Song, y G. Wei, «A 3-kW Wireless Power Transfer System for Sightseeing Car Supercapacitor Charge», IEEE Transactions on Power Electronics, vol. 32, n.º 5, pp. 3301-3316, may 2017, doi: 10.1109/TPEL.2016.2584701.

[5] R. L. Steigerwald, «A comparison of half-bridge resonant converter topologies», IEEE Transactions on Power Electronics, vol. 3, n.º 2, pp. 174-182, abr. 1988, doi: 10.1109/63.4347.

[6] Y. Ye, C. Yan, J. Zeng, y J. Ying, «A novel light load solution for LLC series resonant converter», en INTELEC 07 - 29th International Telecommunications Energy Conference, sep. 2007, pp. 61-65, doi: 10.1109/INTLEC.2007.4448738.

[7] W. Zhang, S. C. Wong, C. K. Tse, y Q. Chen, «Analysis and Comparison of Secondary Series- and Parallel-Compensated Inductive Power Transfer Systems Operating for Optimal Efficiency and Load-Independent Voltage-Transfer Ratio», IEEE Transactions on Power Electronics, vol. 29, n.º 6, pp. 2979-2990, jun. 2014, doi: 10.1109/TPEL.2013.2273364.

[8] W. Li, H. Zhao, J. Deng, S. Li, y C. C. Mi, «Comparison Study on SS and Double-Sided LCC Compensation Topologies for EV/PHEV Wireless Chargers», IEEE Transactions on Vehicular Technology, vol. 65, n.º 6, pp. 4429-4439, jun. 2016, doi: 10.1109/TVT.2015.2479938.

.[9] C. Cai et al., «Design and Optimization of Load-Independent Magnetic Resonant Wireless Charging System for Electric Vehicles», IEEE Access, vol. PP, n.º 99, pp. 1-1, 2018, doi: 10.1109/ACCESS.2018.2810128.

[10] R. L. Lin y C. W. Lin, «Design criteria for resonant tank of LLC DC-DC resonant converter», en IECON 2010 - 36th Annual Conference on IEEE Industrial Electronics Society, nov. 2010, pp. 427-432, doi: 10.1109/IECON.2010.5674988.

[11] P. Villegas, J. Martín-Ramos, J. Díaz, J. Martínez, M. Prieto, y A. Pernía, «A Digitally Controlled Power Converter for an Electrostatic Precipitator», Energies, vol. 10, n.º 12, p. 2150, dic. 2017, doi: 10.3390/en10122150.